AN ITALIAN SAMPLE OF HIGH RESOLUTION OPTICAL ACTIVITIES

V. Biliotti, D. Bonaccini, G. Brusa, M. Carrabba, M. Cecconi, S. Esposito, M. Gatti, E. Marchetti, and R. Ragazzoni

Astronomical Observatory of Arcetry (Firenze)
Department of Astronomy of Bologna
Center for Studies and Activities for Space, University of Padova
Department of Astronomy, University of Firenze
Astronomical Observatory of Bologna
Department of Astronomy, University of Padova
Astronomical Observatory of Padova
Received December 13, 1993

Some Italian works in the field of high resolution optics, from wave front sensor simulation to space sub–systems, are briefly presented here. A successful tip–tilt correction achieved in laboratory is presented together with a simulation study of the expected performances of a Shack–Hartmann wave front sensor. Furthermore some stellar speckle interferometry experience and the design work of a cophasing module for a solar space interferometer are briefly given.

INTRODUCTION

In this paper a number of activities held in Italy in order to improve the angular resolution of astronomical images are outlined.

The interest of Italy in this field arose also for the involvement into two projects of large telescopes: the Galileo telescope (a 3.5 m active optic telescope, close to the NTT–ESO design) to be installed in La Palma, Canarias; and the LBT (Large Binocular Telescope), a 2×8.4 m telescope to be erected in Mt. Graham, USA.

The sub–projects outlined here represent a sample, and not a full coverage, of the various activities.

FIRST RESULTS FROM AN ADAPTIVE OPTICS TIP–TILT LABORATORY CORRECTOR

We report the laboratory results obtained at the beginning of June, 1993 with the second prototype of an Image Stabilization System for Astronomical application. This work is part of the ongoing activities of Arcetri Adaptive Optics Group aimed at the development and realization of Adaptive Optics System for 3.5 m GALILEO and 8.4 m LBT telescopes.

The system prototype is based on a P.I.3 piezo fast steering mirror and a four quadrant silicon photodiode (Q–Cell) Tip–tilt sensor.

First we have developed a seeing generator in order to test the performances of our system in the lab. To characterize the statistics of spatial distribution of refraction index fluctuations, we have determined the Modulation Transfer Function of the seeing generator and from this we derived a phase structure function that agrees with a Kolmogorov turbulence. From some measurements of the temporal behavior of image centroid we have obtained the power spectral density of one–dimensional image motion that agrees with the expected theoretical behavior (Fig. 1).

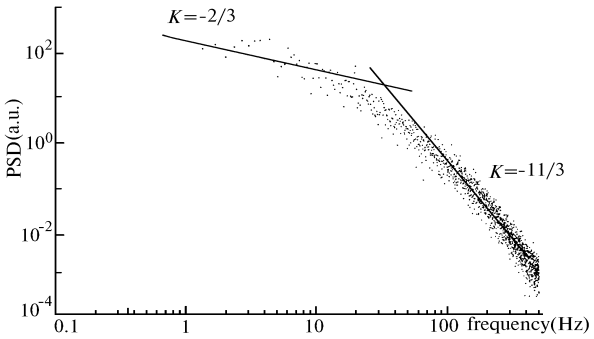

FIG. 1. Power spectral density for one–dimensional image motion.

After a mechanical and electronical compensation of the open loop transfer function of each channel of the system, in order to match the atmospherical tip–tilt perturbation power spectral density, we have closed the loop and tested the performances of the image stabilizer on the optical bench using our seeing generator. Results of the long–exposure point spread function (PSF) are shown in Fig. 2 for these cases: no compensation, compensation of one–axis image motion only, and, for comparison, simulated results for the one–axis case.

A summary of the parameters and results for this experiment is given in Table I.

0235-6880/95/03 182-04 $02.00

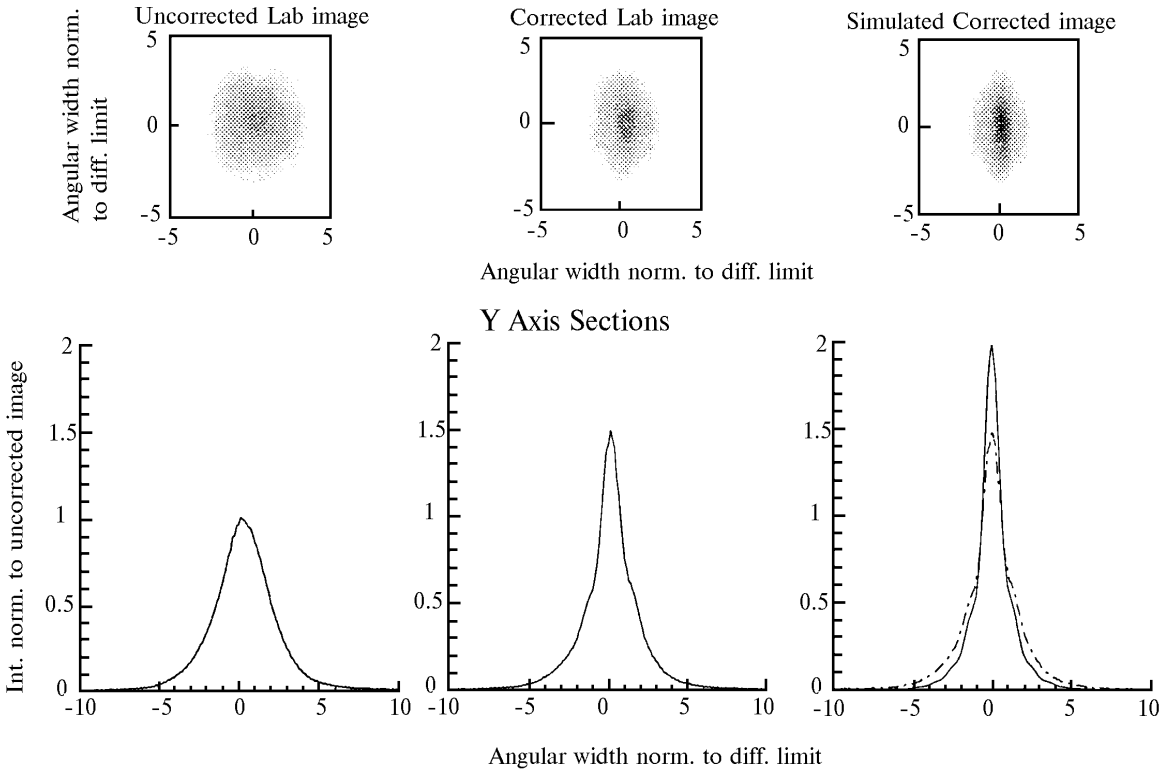

FIG. 2. Various long–exposure point spread functions (PSFs).

TABLE I. Parameters and results for the Tip–Tilt correction experiment.

Parameters	Results
Aperture diameter: 1.5 cm	$FWHM_{Uncorrected} \approx 3.4 \times FWHM_{diffraction}$
$r_0 = 0.44$ cm	$FWHM_{Corrected} \approx 1.7 \times FWHM_{diffraction}$
$DC_{Gain} = 60$	$FWHM_{Simulated} \approx 1.5 \times FWHM_{diffraction}$
f_{3dB}=20 Hz	$SNR_{Corrected}/SNR_{Uncorrected} \approx 1.5$ (Laboratory)
Exp. time = = 30 sec.	$SNR_{Corrected}/SNR_{Uncorrected} \approx 2.0$ (Simulation)

The Q–cell tip–tilt sensor will be upgraded soon in two different ways, with four avalanche photodiodes and with the collaboration of F. Roddier group with a 13–elements curvature wave front sensor.

SIMULATION OF SHACK–HARTMANN WAVE FRONT SENSING

Wave front sensing is a peculiar stage both of Active and Adaptive Optics systems. The simulation of a Shack–Hartmann wave front sensor, and a number of experiments made at the optical bench and at the telescope, leads to a complex code, capable to describe the Shack–Hartmann behavior in a great details, comprising tolerances and misalignments during the manufacturing of the wave front sensor itself.

In Fig. 3 the true arrangement of a Shak–Hartmann is sketched.

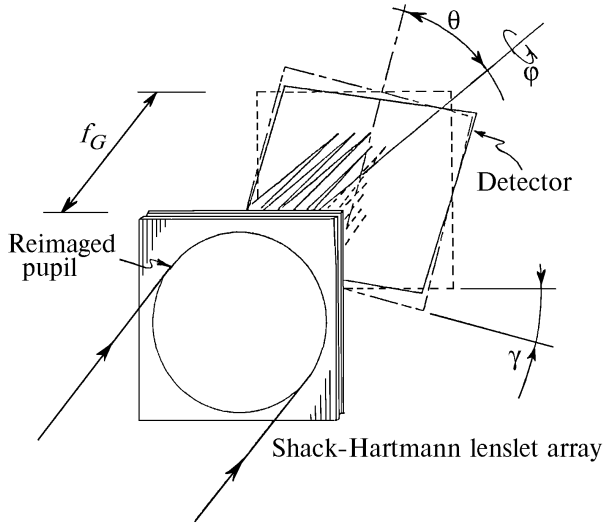

FIG. 3. Detailed arrangement of the detector with respect to the Shack–Hartmann lenslet array.

While for the active optics operations there is need for a very accurate estimation of the wave front, in the case of adaptive optics much more attention has to be paid to the computational speed and rejection of noise.

Following this simple prescription a number of numerical experiments were performed, adding noise of various statistical type and fitting the measurements through a number of solving algorithms. Emphasis was also given on the inversion of the matrix, often ill–conditioned, that is obtained during the process of solving the differential equation governing the Shack–Hartmann behavior.

SOME SPECKLE INTERFEROMETRY EXPERIMENT

The experiment was performed at the 122 cm telescope of the Astrophysical Observatory of Asiago together with Prof. C. Barbieri.

The speckle camera employed for the observations is constituted by a magnification system coupled with a one stage intensified TV camera for the imaging. The images coming from the camera are recorded on a magnetic tape (VHS) with a normal videorecorder. Several runs have been made on a sample of selected binary stars with separation under the arcsecond. The calibration of determining the scale and the orientation of the field of view was performed with two large binary stars. The bandwidth of the filter used is 54.4 nm centered at 589.5 nm. The integration time is fixed at 40 ms, equal to the frame exposure time in the VHS system.

The images were digitized by a specified software for Personal Computer, Screen Machine© of the Fast Electronic GmbH. The digitization format is about 256×256 pixels with a dynamic range of 8 bits (256 gray levels). For each object a great number of sequential frames from the magnetic tape was digitized.

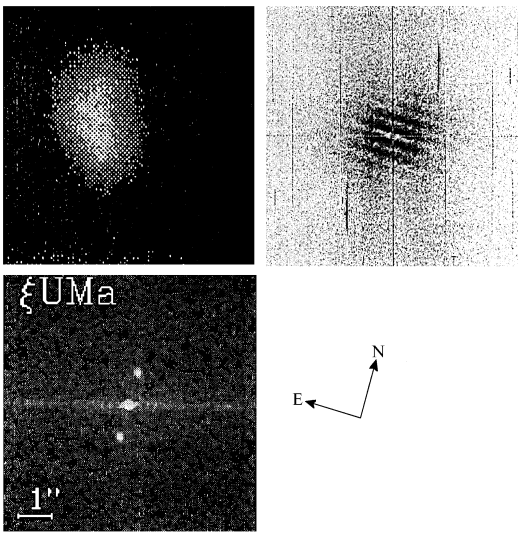

FIG. 4. One specklegram, the power spectrum, and the autocorrelation function of ξ UMa.

The data processing was performed with IDL, Interactive Data Language of the Research Systems, Inc.. We computed the power spectrum of the image of the object dividing the sum of the power spectra of the object's images for the speckle transfer function of a reference star. Operating the FFT of the power spectrum we obtained the autocorrelation function for the distribution of the luminous intensity of the object on the image plane. With this technique we resolved three close binary stars ξ UMa, 10 UMa, and ε Hya; the characteristic of these system are shown in Table II.

The binary ε Hya has a separation very close to the diffraction limit of the telescope (0.″1) and this result shows the effective system performances. In the case of 10 UMa the great magnitude difference ($\Delta m \simeq 2.07$) between the two stars was an hard test bench for the low dynamic range of digitization and the camera detection limits.

TABLE II. Statistical parameters for the three resolved binary stars; the last row indicates the grade of knowledge of the orbit.

	ε Hya	10 UMa	ξ UMa
Cat. Ref.	ADS 6993	DM +42°1956	ADS 8119
Δm	0.9	2.07	0.5
Period (years)	15.076	21.850	59.840
a(″)	0.2520	0.6190	2.5300
e	0.690	0.150	0.414
i(°)	49.3	134.8	122.65
ω(°)	264.0	210.0	127.53
Ω(°)	109.3	22.8	101.59
Grade	1	2	1

Note: Δm is the difference between the two stars; a is angular separation between two stars; e is orbital eccentricity (0 – circular orbit, 1 – parabolic orbit); i is declination of orbit over line of sight (in degrees); and, Ω is parallax angle (in degrees).

TABLE III. Separation and position angle for ξ UMa, 10 UMa, and *ε Hya.*

Object	Separation (″)	PA(°)
ξ UMa,	0.88±0.02	355.5±1.5
Ephem. (1993.15)	0.86	356.38
10 UMa	0.46±0.05	183.9±6.2
Ephem. (1993.15)	0.52	192.04
ε Hya	0.20±0.05	147±14
Ephem. (1993.15)	0.21	128.55

Shown in Table III are the separations and the position angles obtained from the autocorrelation functions.

COPHASING SYSTEM FOR A SPACE INTERFEROMETER

One of the crucial point of the correct working of an interferometer is its cophasing, that is, the real-time active control of the condition

$$\Delta(\mathrm{OPD}) \ll \lambda , \qquad (1)$$

where Δ indicates finite time variation, OPD is the optical path difference between every pair of telescopes in the array, and λ is the minimum wavelength of the spectral band of the detected real image. In fact, if the above conditions were fulfilled, the real image (consisting in a fringe pattern) would be frozen on the focal plane and then deconvoluted to achieve the final high spatial (~ 0.035 arcsec at λ = 121 nm) and temporal (< 1 s) resolution of image of the observed object.

The MUST (multimirror ultraviolet solar telescope) cophasing system (CS hereafter) is conceptually similar to the SUN (solar ultraviolet network) one but is contained in a ∅ 300×100 mm cylindrical box placed under the primary mirror of the Ritchey–Chretien recombination telescope (see Fig. 5) which focalizes the five beams, coming from the entrance pupil of the array, in the center of the ~∅ 20 mm plane mirror *16* (see Fig. 6). A~ ∅ 2 mm pinhole in *16* lets the light corresponding to a ~ 30 arcsec sky field of view (FoV hereafter) enter in the focal instrumentation while the residual FoV (a 30–300 arcsec corona) is reflected towards the CS.

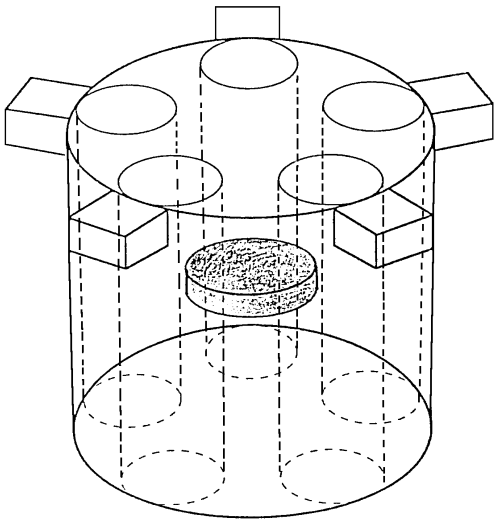

FIG. 5. Collocation of the CS in MUST.

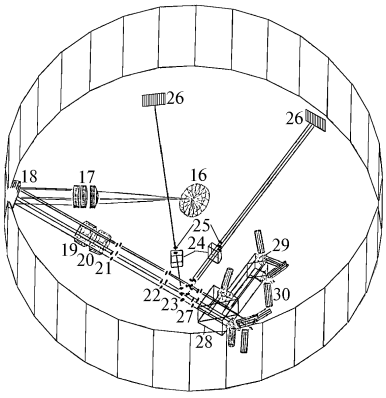

FIG. 6. Sketch of the MUST CS.

A ~ F/8, ~ ∅ 27 mm lens assembly *17*, forming an afocal optical system together with the recombination telescope, collimates the five beams. Then, they are reflected by the ~ 20×20×5 mm plane mirror *18* towards the two achromatic rotating wedges *19–20* which make it possible to move an high contrast FoV region of the high beams on the axis of the following optical system to pre-aligne telescopes (ray-tracing simulations of the lens and wedge assembly have just been begun). The lens sets *21–22* focalize and adjust a~30 arcsec portion of the selected FoV on the small plane mirror set *23* pin-holes, wide enough to let through a FoV corresponding to a single telescope Airy disk (~ 20 arcsec at λ = 121 nm). The residual FoV (a 0.25–30 arcsec corona) is reflected towards the pre-aligned optical system *24–25–26*, one for two beams and another for the other three, ending with CCD where each FoV is compared to the others. A pointing precision of ~ 0.1 arcsec is expected with such a system sending fine corrections to the secondary mirrors. With finer corrections, improving the fringe contrast of the interference pattern on the focal plane while cophasing the system, a~ 3 mas final pointing precision is expected.

The beams crossing the pinholes *23* are then recollimated by the lens set *27* and used, two by two via beamsplitter prisms assembly *28*, in reference interferometers *29-30* where a synchronous detection technique allows white light fringe tracking. The small cylinders *30* include Brewster plate polarisers, which increase the fringe contrast, and SiO diodes to measure the light flux. The real-time white fringe tracking is used to generate a corrective delay line signal. A fulfilment of condition Δ (OPD) < $\lambda/10$, (λ = 121 nm) is expected with such a system.

A laboratory experiment, to detect red laser and then white light fringe, has been conceived as shown in Fig. 7. An application of this dispositive on the 120 cm "Galileo" telescope of the Asiago Observatory is foreseen. Results of this experement will be given in a future paper.

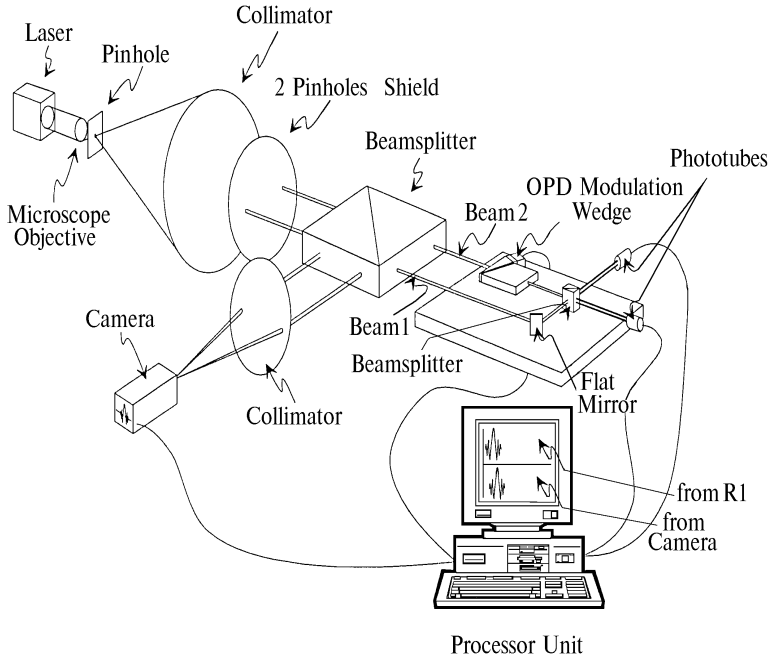

FIG. 7. A sketch of the laboratory experiment conceived to detect the red laser and then white light fringe between two beams.